

Three-particle quantum correlation interferometry

F.V. Kowalski

Physics Department, Colorado School of Mines, Golden CO. 80401 U.S.A.

A three-body quantum correlation is calculated for two particles reflecting from a mirror. Correlated interference, a consequence of conservation of energy and momentum, occurs for states in which the order of reflection is indeterminate. The resulting quantum joint probability density function exhibits interference with diverse characteristics, depending on the coherence lengths of the substates. Marginal probability density functions can contain information about the quantum nature of all three bodies, even if only one particle is measured. Microscopic particles reflecting from a mesoscopic or macroscopic mirror are used to illustrate unique features of this three-body correlation interferometry. The microscopic momentum exchanged then generates mirror substates which interfere to produce quantum effects which do not vanish with increasing mirror mass, while the small displacement between these mirror states can yield negligible environmental decoherence times.

PACS numbers: 03.65.Ta, 03.65.-w, 03.75.Dg, 03.75.-b

Multiparticle interferometry reveals a different aspect of quantum mechanics. This is manifest both as many-body coincidences, which depend on the number of paths and/or the number of particles within such an interferometer [1], and in the resulting marginal probability density functions. For bipartite systems, using photon pairs generated by parametric downconversion, various interferometer paths have been used [1–4]. However, experimental confirmation of quantum predictions is more difficult to obtain for similar systems with non-zero rest mass particles.

Scarcer yet are examples of three-body interferometers traversed by non-zero rest mass particles, although gedanken-experiments (typically using identical particles) have been discussed [1, 5]. This is perhaps due to a combination of few exact solutions for three-body systems and the difficulty in constructing three-body beamsplitters.

Here, both a three-body beamsplitter and interferometer are described using three distinguishable non-zero rest mass particles. The splitting mechanism involves elastic reflection in one dimension. By increasing the number of interacting particles, this reflection process can act as a beamsplitter or interferometer for even more particles. Measurements of particle reflection, but not associated with interference, have involved mirrors that reflect atoms [6] and Bose-Einstein condensates [7], atoms reflecting from a solid surface [8], neutrons [9] and atoms [10] reflecting from vibrating mirrors, and atoms reflecting from a switchable mirror [11].

Fig. 1 shows schematic representations of this 3-body state splitting process. Actual three-body quantum joint probability density functions, PDFs, are described later. The particle substate PDFs, before interaction, are the Gaussians at $t = -\tau$, one of which, to the left of the ‘mirror’, is moving to the right, while the other, to the right of the ‘mirror’, is moving to the left. The ‘mirror’ is represented as the black rectangle, moving to the right. These are referred to as particle 1, the mirror, and particle 2, with masses m_1, M, m_2 , initial velocities v_1, V, v_2 , and coordinates x_1, X, x_2 , respectively.

At $t = 0$ interference between the incident and reflected particle substates is shown as oscillations in the PDF, while interference between the mirror substates, which have and have not reflected the particles, is represented by the rectangular checkerboard pattern rather than the solid rectangle. This snapshot at $t = 0$ illustrates a region of correlated interference, although the correlation cannot be shown in such a simple schematic. These quantum correlations in the three-body interference, a consequence of conservation of energy and momentum, are manifest as coincidence rates, e.g. a correlation in the measurement of the positions of the particles and mirror. A null in the PDF, as a function of the three coordinates (not shown in this schematic), is an example of a correlation where all three objects cannot be observed. At time $t = \tau$ the three wavegroups have separated so that no overlap occurs. The expectation value of the position of each wavegroup substate then obeys the laws of classical reflection.

Fig. 1, at $t = 0$, illustrates an ‘open-interferometer,’ where the phase difference, which determines interference, depends on the spatial locations and times of measurement of each particle in the multiparticle system. A one-particle example of such an open interferometer is the region behind a double slit, where the detector’s output depends on its location. The phase difference in a closed interferometer, such as a one-particle Mach-Zehnder, depends on its fixed path difference and is independent of the detector location beyond the output port. A gedankenexperiment for a three-particle closed interferometer is found in reference [1].

Detection of the three objects, in fig. 1, can then occur at different times and locations, yielding asynchronous correlation interferometry [12]. To determine the PDF in such a case, assume a noise-free and non-destructive measurement of particle 1 first, collapse of its particle substate, and later sequential measurements of the mirror

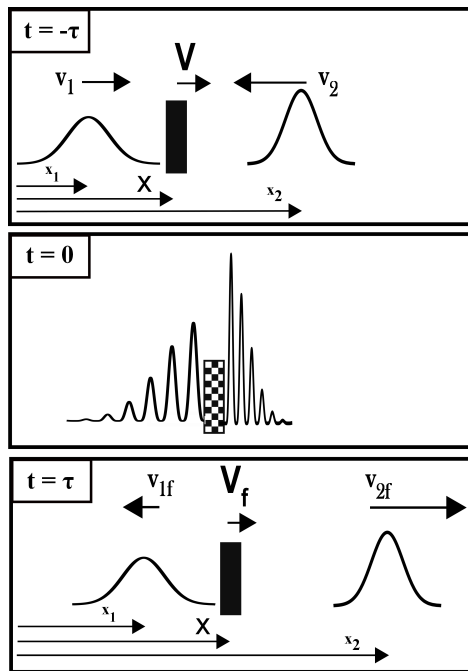


FIG. 1: 3-body reflection schematic.

and particle 2, while no interaction occurs between the collapsed state of each measured body with the remaining unmeasured bodies.

To predict such effects, assume that the two particles and mirror are initially in an uncorrelated eigenstate of energy before reflection. The three-body Schrödinger equation for reflection is then solved for the energy eigenstates. Wavegroups, as sketched in fig. 1, are formed from a superposition of these solutions. The particle-mirror interaction is modeled as a moving delta function potential where reflection is assumed to occur at the center of mass of the mirror, with the boundary condition that the wavefunction (incident and reflected states) vanish at $x_1 = X = x_2$.

The energy eigenstate solution is then parsed (using conservation of energy and momentum in reflection) to completely separate the variables associated with the particles and mirror from each other [12]. In doing so, time parameters t_1 , T , and t_2 are introduced. These are coefficients of the energy in the wavefunction's phase for particle 1, the mirror, and particle 2, respectively. They also label the different times at which the particle and mirror are measured.

The different time labels do not indicate evolution of the subsystems via different Hamiltonians as do the different time variables used by McGuire [13] nor are they used to generate a manifestly Lorentz invariant theory as done by Petrat [14]. They neither tick at different rates nor are they out of phase, but rather they act as only a label to isolate the effect of the energy of each body in the phase of the 3-body wavefunction. Then, when particle 1 is measured at position x_1 and time t_1 , only its parameters are fixed, while those of the mirror and particle 2 continue to evolve in time until a sequential measurement is made on them. The later measurements on the mirror and particle 2 are done under the same assumptions as for the first measurement. The resulting PDF is a function both of the different particle positions and different times at which each is measured [12].

Consider next the energy eigenstates for the system shown in fig. 1. These three bodies can exist in 6 possible eigenstates: **(1)** uncorrelated incident, **(2)** particle 1 has reflected but not particle 2, **(3)** particle 2 has reflected but not particle 1, **(4)** particle 1 reflected first followed by reflection of particle 2, **(5)** particle 2 reflected first followed by reflection of particle 1, and **(6)** simultaneously reflection of the three bodies. Since it is not known where the bodies are located for energy eigenstates, these six 'paths' must be superposed.

Interestingly, conservation of energy and momentum do not determine a unique solution for simultaneous 3-body elastic reflection [15]. It is assumed here that the probability for such a collision is small compared with that of the other five 'paths' and therefore is neglected [16]. Experimental confirmation of the resulting predictions will validate this assumption.

Analytic results are typically too lengthy to present. However, in the limit $M \gg (m_1, m_2)$, the PDF for the

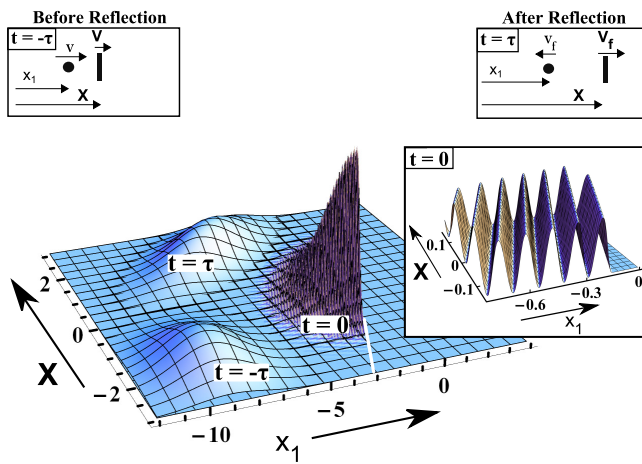


FIG. 2: Three sequential two-body joint probability density snapshots vs coordinates (x_1, X) for reflection only of particle 1 from the mirror. The lower PDF waveform moves toward the diagonal white line, corresponding to $x_1 = X$, then reflects in the middle snapshot where the incident and reflected two-body wavefunctions ‘overlap’, and finally it moves away from the diagonal in the upper snapshot. The upper left inset is a schematic of the ‘classical’ analog before reflection while the upper right inset is that after reflection. The middle right inset is a magnified version of the $t = 0$ plot. There is no classical analog for the middle snapshot. The white line corresponds to $x_1 = X$.

wavefunction, which is the sum of these energy eigenstates, reduces to

$$PDF_{eigenstate}^{energy} \propto \frac{3}{2} - \cos(\alpha) + \frac{\cos(\alpha + \beta)}{2} - \cos(\beta), \quad (1)$$

with

$$\alpha = \frac{2m_1(V - v_1)(V(t_1 - T) + x_1 - X)}{\hbar}$$

$$\beta = \frac{2m_2(V - v_2)(V(T - t_2) + X - x_2)}{\hbar}.$$

Note that the parameters of the three bodies are coupled in this interference expression. The result for a simultaneous measurement is given by setting $t_1 = T = t_2$.

Any experimental realization of such an interferometer will involve wavegroups, which are formed by summing over these energy eigenstates for Gaussian distributions of the initial velocities of the mirror and particles. An analytic expression for a 3-body wavegroup can be obtained if all three are measured simultaneously. The results presented below involve this simplification [17].

Fig. 2 is used to show the PDF for reflection of *only* particle 1 from the mirror. This is represented schematically in fig. 1 by eliminating the particle 2 substate.

It is difficult to display PDF plots of correlated interference, as shown schematically in the middle snapshot of fig. 1, when particle 2 also reflects. Instead, these plots are shown as a function of only the coordinates of particle 1 and the mirror, for a fixed position of particle 2. Another simplification, to illustrate such 3-body PDFs, incorporates a broadband mirror substate wavegroup (narrow spatial width compared with the fringe structure) with narrow band (large spatial width compared with the fringe structure) particle substate wavegroups. The interferometric effects of the addition of the third body, are then shown in fig. 3. The only difference between the upper and lower two plots in fig. 3 is the value of x_2 . In both plots, x_2 is fixed to be within the position of interferometric PDF oscillations sketched in fig. 1. The lower horizontal ridge along the x_1 axis corresponds to a superposition of the incident wavegroup with and without reflecting particle 2. The diagonal oscillations in the PDF correspond to a superposition of paths (2), (4), and (5), which are defined above. This is a manifestation of the 3-body interferometer.

A PDF plot of reflection only of particle 1 from the mirror, with the same parameters as used in the upper and lower plots of fig. 3, is shown in the inset at the middle of fig. 3. Only two PDF ridges appear, with no oscillations. However, there is no 2-body interference, as shown in the middle snapshot of fig. 2, since the short spatial width of the mirror wavegroup substate, relative to its recoil distance, results in distinguishable two-body states (the mirror has reflected the particle in the upper but not the lower PDF ridge).

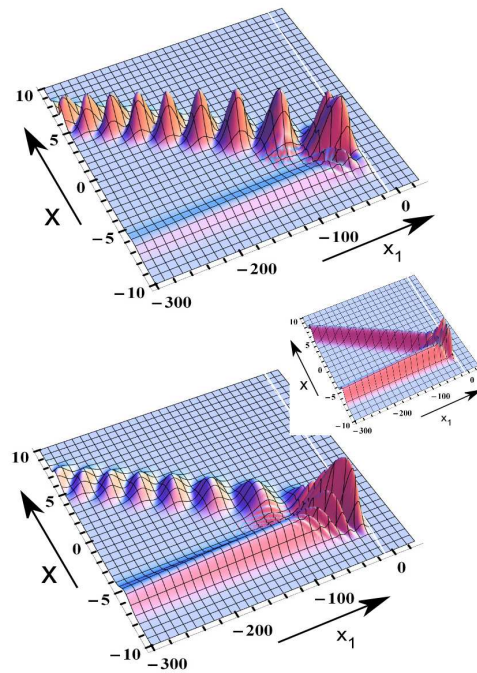


FIG. 3: The upper and lower 3-body PDF correlated interference plots differ only by the particular value used for x_2 . All other parameters in these plots are the same. The inset is the 2-body PDF plot for reflection only of particle 1 from the mirror.

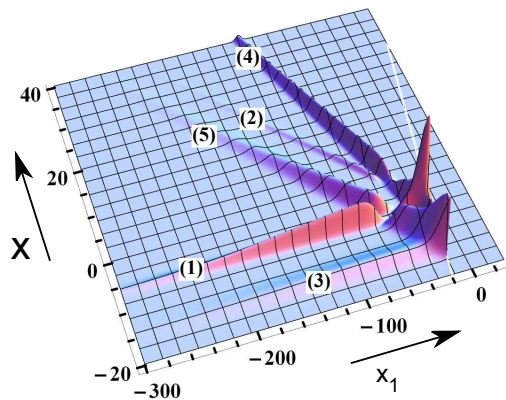


FIG. 4: Fig. 3 has been modified by increasing m_2 and decreasing the spatial width of the mirror. The paths associated with the separate ridges are labeled as described in the text. The lack of overlap eliminates the interference in fig. 3.

Fig. 4 illustrates reflection acting more as a beamsplitter than an interferometer. This is accomplished by narrowing the spatial width of the mirror substate wavegroup while also increasing the mass of particle 2, relative to the parameters used in fig. 3. The reflection of particle 2 then imparts sufficient momentum to separate these narrower wavegroups, thereby eliminating the interference shown in fig. 3. For example, the two interfering states parallel to the x_1 axis of fig. 3 no longer overlap in fig. 4. For a measurement of particle 1 at x_1 and particle 2 at the value used in the figure, the mirror is split into 5 distinct positions along the ridges, each associated with a path, labeled numerically, as defined above. Although the different paths no longer overlap, this is not a separable state.

Verification of such correlated interference requires simultaneous measurement of both particles and the center of mass of the mirror with instruments having a spatial resolution smaller than the fringe spacing. For a static

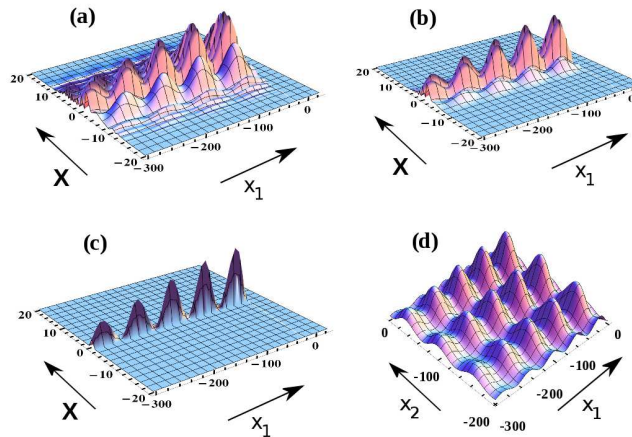


FIG. 5: PDF plots for $M \gg (m_1, m_2)$. (a) through (c) fix x_3 and the particle coherence lengths while the mirror coherence length decreases. Part (d) illustrates the marginal PDF derived from part (c).

mirror reflecting microscopic particles and $M \gg (m_1, m_2)$, this spacing is about half the deBroglie wavelength of the particles, which at $\sim 1 \mu\text{m}$ for ultracold atoms [18], potentially satisfies this requirement. Additionally, the effects of the longitudinal coherence length, l_c , need to be considered. For ultracold atoms $l_c \leq 10 \mu\text{m}$ [18], while for a mirror this is given by $l_c \approx \lambda^2/\Delta\lambda = \lambda V/\Delta V$ [19]. If the uncertainty in the mirror velocity is determined by its thermal equilibrium with the environment then $\Delta V_{thermal} \approx \sqrt{2k_B T/M}$ yielding for the mirror, $l_c^{thermal} \approx h/\sqrt{2Mk_B T}$.

To illustrate the effect of varying the mirror coherence length, a sequence of decreasing coherence lengths for the mirror is shown in figs. 5 (a), (b), and (c). Only the particle masses have been decreased, relative to those used in fig. 3, to generate interference similar to that shown in the middle snapshot of fig. 2.

Measuring correlations among fewer bodies is more practical. To predict such results, the many-body PDF is integrated over the coordinates of one or more of the bodies, appropriately reducing the coordinate space that the PDF spans and yielding a marginal PDF [5]. For example, integrating over the mirror coordinate reduces $PDF(x_1, \mathbf{X}, x_2)$ to $PDF(x_1, x_2)$. This procedure, when applied to the PDF shown in fig. 5 (a), virtually eliminates interference. Yet, for the conditions illustrated in fig. 5 (c), this leads to the marginal $PDF(x_1, x_2)$ shown in fig. 5 (d).

For these long coherence length particle substates and the short coherence length mirror, this marginal PDF can be approximated, using the simultaneous version of eqn. 1, with the mirror substate being a delta function distribution in position, peaking at $\mathbf{X} = \mathbf{X}_0$. Integrating over the mirror coordinate then yields $PDF_{eigenstate}^{\int \dots d\mathbf{X}}(x_1, x_2) = PDF_{eigenstate}^{energy}(x_1, \mathbf{X}_0, x_2)$. This differs from the result shown in fig. 5 (d) by a slight variation in the magnitude of the PDF due to the large but finite particle coherence lengths.

A comparison of $PDF_{eigenstate}^{\int \dots d\mathbf{X}}(x_1, x_2)$ can be made with independent one-body solutions to the Schrödinger equation with $M \gg (m_1, m_2)$ (one solution for each particle residing on opposite sides of the mirror) while treating the mirror as a classical potential. The resulting PDF, with $\mathbf{X} \rightarrow \mathbf{X}_0$ in α and β ,

$$PDF_{mirror}^{classical}(x_1, x_2) \approx 2 - \cos(\alpha) - \cos(\beta), \quad (2)$$

differs from the approximate marginal PDF by not having the correlation term $\cos(\alpha + \beta)$ (which adds a phase shift and a variation in the magnitude of the PDF as a function of position). A measurement might then consist of ultra cold atoms reflecting from opposite sides of a stationary mirror. Observation of a standing wave atom PDF pattern, with the correlation term, would then indicate quantum behavior of the mirror without a direct measurement of it.

While the approximation using eqn. 1 is useful in understanding how the interaction of the three bodies is manifest in a marginal PDF, it is incomplete for short coherence length particle substates since both the time dependent motion of the wavegroup and its spatial dependence are neglected. It is most accurate during overlap of the wavegroups.

The coordinate space of $PDF(x_1, x_2)$ can again be lowered by reducing the coherence length of particle 2, resulting in a sequence for fig. 5 (d) which progresses in a similar manner to fig. 5 (a) going to fig. 5 (c). The particle 2 substate then becomes a delta function distribution in position, peaking at $x_2 = x_{20}$ while that of particle 1 remains in a broad spatial distribution. This one body PDF can again be approximated by integrating $PDF_{eigenstate}^{\int \dots d\mathbf{X}}(x_1, x_2)$

over x_2 yielding,

$$PDF_{eigenstate}^{f \dots dX dx_2}(x_1) \propto \frac{3}{2} - \cos(\alpha) + \frac{\cos(\alpha + \beta)}{2} - \cos(\beta), \quad (3)$$

with $X \rightarrow X_0$ and $x_2 \rightarrow x_{20}$ in α and β .

Such a result is useful in estimating the 3-body correlation effects in the one-body marginal PDF. However, the approximation again neglects the time evolution and spatial dependence of the wavegroup substates. The validity of this approximation then rests on the order of reflection being indeterminate. The long duration of the particle 1 interaction mitigates this constraint.

If, on the other hand, the particle 2 wavegroup reflects before or after any interaction of particle 1 with the mirror, then the result is the one-body solution to the Schrödinger equation, $PDF_{mirror}^{one\ body}(x_1) \propto 1 - \cos(\alpha)$. This differs from the 3-body result given by eqn. 3.

By measuring neither the mirror nor particle 2, evidence of 3-body superposition can therefore be retained in the measurement of the standing wave PDF of only particle 1. Such a measurement might consist of a nearly static mirror in a system with coherence lengths $l_c^M \ll l_c^{m_2} < l_c^{m_1}$. A fixed delay of particle 2 (constant β due to a fixed $x_2 - X$) is introduced. The interaction time of particle 1 must be longer than the transit time of particle 2 to the mirror for the order of reflection to remain indeterminate. Observation of the correlation term in only the standing wave PDF pattern for particle 1, as a function of $x_1 - X$ (and therefore α), would then indicate quantum behavior of the mirror.

Correlation interferometry in reflection has advantages in measuring many-body quantum effects both on systems composed of 3 or more bodies and on mirrors of increasing mass. There is neither the alignment nor the path length sensitivity found in division of amplitude or wavefront interferometers, while the beamsplitting mechanism requires only that the order of reflection be indeterminate. It is therefore of interest to determine the upper limit on the mirror mass, in observing quantum correlation effects.

Macroscopic superposition states have been of concern since early in the development of quantum mechanics. To understand why such states can potentially be observed, some assumptions about arguments against such observations need to be challenged in relation to the example treated here. A summary, including results from more detailed treatments on two-body reflection [12, 17], is: (1) The mirror fringe spacing does not shrink as its mass increases due to the superposition of mirror states which differ only by the microscopic momentum exchanged with the particles. (2) Interferometric quantum correlation is a requisite in satisfying conservation of energy and momentum in reflection [17]. (3) The difference in wavevectors of the interfering macroscopic mirror substates, due to reflecting microscopic particles, divided by the spread in wavevectors, of which the mirror substate is composed due to thermal motion, is the ratio R . Optical wavegroups with R values similar to a microscopic particle reflecting from a macroscopic mirror have been shown to exhibit interference. (4) Decoherence of the macroscopic superposition via interaction with the environment increases exponentially with the spatial separation of these states [20]. The small separation of these interfering macroscopic mirror states, having reflected microscopic particles, mitigates such decoherence. (5) Many-body quantum effects are maintained for short mirror coherence lengths, even in the marginal PDF, as shown above.

Only a small set of parameters and interferometric geometries have been explored here. Other possibilities include closed interferometers, such as a thin aluminum film generating reflections of a neutron from both its surfaces [12]. Such interference is not transient for two main reasons: first the reflected pulses from each thin film surface maintain overlap as they both travel in the backward direction and second they have the same Doppler shift (reflecting from interfaces moving at the same speed). Reflection of two neutrons from such a film is potentially a more feasible extension of the 3-body correlated interference work described here. Asynchronous measurement can also mitigate transient effects [12].

Reflection of atoms from mirrors has been previously studied, but not in treating both the particle and reflector as quantum objects, nor in the mesoscopic reflector mass regimes considered here, nor in an attempt to measure the resulting ‘standing-wave’ interference. There exist few examples of 3-body quantum correlated interference for non-zero rest mass particles. Verification of the above predictions, even in the microscopic regime for both particles and mirror, is therefore of fundamental interest. Although neither comprehensive nor intended as an experimental proposal, these results indicate a direction, heretofore unexplored, for further research in understanding many body quantum correlation and extending quantum measurements to larger masses.

[1] D. M. Greenberger, M. A. Horne, and A. Zeilinger, *Physics Today* **46** 22 (1993).

- [2] D.Franson, Phys.Rev.Lett., **62** 2205, (1989).
- [3] J-W. Pan, D. Bouwmeester, M. Daniell, H. Weinfurter, and A. Zeilinger, Nature, **403** 515, (2000).
- [4] J-W. Pan, Z-B. Chen, C-Y. Lu, H. Weinfurter, A. Zeilinger, and M. Żukowski Rev. Mod. Phys. **84**, 777.
- [5] K. Gottfried, Am. J. Phys. **68** 143 (2000).
- [6] D. Kouznetsov and H. Oberst, Phys. Rev. A **72**, 013617-1 (2005).
- [7] T. A. Pasquini, M. Saba, G.-B. Jo, Y. Shin, W. Ketterle, and D. E. Pritchard, Phys. Rev. Lett. **97**, 093201-1 (2006).
- [8] F. Shimizu, Phys. Rev. Lett. **86**, 987 (2001).
- [9] T. Hils et. al., Phys. Rev. A **58**, 4784 (1998).
- [10] Y. Colombe, B. Mercier, H. Perrin, and V. Lorent, Phys. Rev. A **72**, 061601 (2005).
- [11] Szriftgiser, P., D. Guery-Odelin, M. Arndt, and J. Dalibard, Phys. Rev. Lett. **77**, 4 (1996).
- [12] A two-body treatment of asynchronous measurement in reflection is found here: Kowalski, F.V. and R.S. Browne, arXiv:1405.0031
- [13] J.H. McGuire and A.L. Godunov, Phys. Rev. A, **67** 042701 (2003).
- [14] S. Petrat and R. Tumulka, Proc. R. Soc. A, **470** 20130632 (2014).
- [15] B. Smith, et. al., ACM Transactions on Graphics (Proceedings of SIGGRAPH 2012), **31**, 186:1 (2012).
- [16] Quantum correlation in a simultaneous 3-body collision is then determined by more than just the conservation laws.
- [17] A two-body treatment of synchronous measurement in reflection is found here: Kowalski, F.V. and R.S. Browne, arXiv:1404.7160
- [18] A. D. Cronin, J. Schmiedmayer, and D. E. Pritchard, Rev. Mod. Phys. **81**, 1051 (2009).
- [19] M. Ferrero and A. van der Merwe, *Fundamental Problems in Quantum Physics*, p-125 (Kluwer Academic Publishing, Dordrecht, 1995).
- [20] W. H. Zurek, Rev. Mod. Phys., **75**, 715, (2003).